

Evolution of charge order through the magnetic phase transition of LuFe₂O₄

M. Bartkowiak,^{1,2} A. M. Mulders,¹ V. Scagnoli,³ U. Staub,³ E. Pomjakushina,⁴ and K. Conder⁴

¹*School of Physical, Environmental and Mathematical Sciences, UNSW, Canberra ACT 2600, Australia*

²*The Bragg Institute, Australian Nuclear Science and Technology Organisation, Lucas Heights NSW 2234, Australia*

³*Swiss Light Source, Paul Scherrer Institut, 5232 Villigen PSI, Switzerland*

⁴*Laboratory for Development and Methods, Paul Scherrer Institut, 5232 Villigen PSI, Switzerland*

(Received 17 May 2012; published 13 July 2012)

The charge order in multiferroic LuFe₂O₄ has been investigated with resonant x-ray diffraction at the Fe K edge in the combined charge ordered and magnetic phase. The energy dependence of the charge order reflection ($\frac{1}{3} \frac{7}{3} \frac{2}{2}$) has been analyzed in detail to investigate the charge disproportionation between the iron sites as a function of temperature. It is found that the charge disproportionation is constant within $0.02e$ across the Néel temperature T_N . The charge order reflection exhibits a decrease in intensity with increasing temperature which is attributed to an increase in the probability of electron hopping. We confirm the increase in polarization at T_N is not of static origin but rather dynamic. Our observations are consistent with antiferromagnetically aligned magnetic moments inhibiting the double exchange mechanism and reducing the probability of electrons hopping between Fe²⁺ and Fe³⁺ in the magnetic phase.

DOI: [10.1103/PhysRevB.86.035121](https://doi.org/10.1103/PhysRevB.86.035121)

PACS number(s): 75.25.Dk, 75.85.+t, 61.05.C-

I. INTRODUCTION

LuFe₂O₄ belongs to the RFe₂O₄ (where R is typically a rare-earth metal) family of compounds, known for their hexagonal layered structure and complex charge and magnetic ordering. These compounds have been shown to undergo charge separation into Fe²⁺ and Fe³⁺ species,^{1,2} while Mössbauer measurements showed that electron hopping occurs between Fe atoms³ and the charge on a specific Fe atom can fluctuate between Fe²⁺ and Fe³⁺ states.⁴ Two-dimensional (2D) magnetic order was shown to appear in YFe₂O₄ (Ref. 5) and YbFe₂O₄.⁶ It was also suggested that the charge and magnetic order in RFe₂O₄ compounds are correlated and magnetoelectric effects should be visible,⁷ following the observations of changes in the dielectric constant of ErFe₂O_{4- δ} depending on the magnetic structure.⁸ In LuFe₂O₄ the charge order (CO) has been shown to be 2D below $T = 500$ K and to extend into a three-dimensional (3D) CO below $T_{CO} \sim 330$ K.⁹ Charge order in LuFe₂O₄ was initially interpreted as polar ordering,¹⁰ following similar findings in manganites¹¹ and nickelates.¹²

LuFe₂O₄ has generated a large scientific interest because its proposed ferroelectric moment caused by frustrated charge order coexists with magnetism near ambient temperature.¹³ LuFe₂O₄ adopts a ferroelectric (FE) ground state below T_{CO} , while below the Néel temperature $T_N \sim 240$ K the Fe magnetic moments order which enhances the FE polarization by 20%. Additionally, electric conductivity of LuFe₂O₄ has been shown to change nonlinearly with voltage, and the nonlinearity is anisotropic.¹⁴ In polycrystalline samples the nonlinearity of electric conductivity has been shown to originate from Joule heating of the sample.¹⁵ It has been demonstrated that the dielectric properties of LuFe₂O₄ can be changed by applying a magnetic field^{16,17} and that pulsed currents can change the magnetic state.^{18,19} It has been debated whether either of the two effects originates from the multiferroic properties of LuFe₂O₄. The magnetic field effect on the dielectric properties has been attributed to Maxwell-Wagner-type contributions from electrical contacts on the sample rather than to intrinsic

properties of the sample itself,²⁰ and the electric current effects can be explained as a result of resistive heating.²¹ The study of LuFe₂O₄ is hampered by the apparent high sensitivity of the charge order and magnetic properties to oxygen stoichiometry.^{15,22,23} At the same time the inherent complexity of the system allows for many different configurations of magnetic moments^{22,24} and of electric charges on Fe atoms.²⁵ In order to adequately describe the charge dynamics in LuFe₂O₄, new theoretical models are being developed.^{26,27}

A second magnetic phase transition that improved the correlation of CO in the c direction was found at $T \sim 175$ K,²⁸ while the magnetic structure peaks broadened indicating an increase in magnetic disorder.²⁵ In a related study, Mössbauer spectroscopy and optical spectroscopy found a decrease in the electron hopping rate with temperature, due to the effective number of d electrons capable of overcoming the energy barrier between Fe²⁺ and Fe³⁺ decreasing with temperature.²⁹

In compounds such as YbFe₂O₄ (Ref. 30) and YFe₂O₄ (Ref. 31), the CO superstructure appears in the form of pancakelike domains, and in YbFe₂O₄ these have been shown to increase in size with cooling.³⁰ Pancakelike CO domains are also present in LuFe₂O₄.³²

The crystal structure of rhombohedral LuFe₂O₄ consists of a triangular double layer of iron ions, with trigonal bipyramids of five oxygen nearest neighbors (n.n.), in which equal amounts of Fe²⁺ and Fe³⁺ populate the iron sites. In a perfectly charge ordered state, each site may be considered as having either an excess or a deficiency of half an electron compared to the average ion valence of Fe^{2.5+}. Alternatively, charge disproportionation with fractional charges may exist as exemplified in nickelates.³³⁻³⁵ In this case the two species are Fe^{2.5+ δ} and Fe^{2.5- δ} , where δ is the additional or missing fractional charge on each Fe ion. We refer to $\delta = 0.5$ as complete charge disproportionation, and to $\delta < 0.5$ as incomplete charge disproportionation.

A possible explanation for the enhanced polarization at T_N in LuFe₂O₄ is that above T_N , $\delta < 0.5$, while below T_N charge disproportionation increases to full charge separation and

$\delta = 0.5$. Resonant x-ray diffraction studies^{23,36} and Mössbauer spectroscopy²⁹ have determined that δ is close to 0.5 at room temperature. A change in disproportionation at T_N is therefore likely to be small. Previously we performed a precise resonant x-ray diffraction (RXD) and determined that the Fe^{2+} orbitals exhibit a glasslike state. Using a self-consistent iteration the anomalous scattering factors of the $\text{Fe}^{2.5+\delta}$ and $\text{Fe}^{2.5-\delta}$ have been determined from the RXD.³⁶ They exhibit a chemical shift of 4.0(1) eV which is close to the chemical shift of 4.5 eV reported for Fe^{2+} and Fe^{3+} in water complexes.³⁷

Recent publications questioned whether LuFe_2O_4 develops FE polarization.^{38,39} An infrared spectroscopy study of lattice dynamics of LuFe_2O_4 suggested antipolar ordering of the bilayers instead of FE.³⁸ Based on x-ray diffraction and x-ray magnetic circular dichroism results, it was proposed³⁹ that within each Fe_2O_4 bilayer both layers exhibit the same electrical charge and the charge neutrality is preserved between pairs of bilayers. The experiment described in this paper cannot verify the correctness of either of the models, as the superstructure reflection that we recorded is present regardless of the FE or antiferroelectric (AFE) ordering of bilayers, and both of the orderings require the Fe^{2+} and Fe^{3+} charge separation. Our treatment of experimental results makes no assumptions as to which Fe sites in the CO supercell are occupied by Fe^{2+} or Fe^{3+} .

In a recent neutron diffraction study using different electric field cooling procedures, we proposed that the increase in ferroelectric polarization at T_N is due to a transition from paramagnetic 2D CO to antiferromagnetic 3D CO in the presence of an applied electric field.⁴⁰ The CO is stabilized by the antiferromagnetic order, preventing electrons from hopping between Fe^{2+} and Fe^{3+} when their magnetic moments are aligned antiparallel. This is consistent with theoretical considerations for layered iron oxides,²⁶ which indicate that CO fluctuates due to thermal hopping of electrons between Fe atoms and is stabilized by the onset of ferrimagnetic order.

In this paper we use RXD to compare the CO in the paramagnetic state with that of the magnetic state. RXD has become a powerful technique for studying charge, orbital, and magnetic arrangements. Tuning the energy of the incoming radiation to an absorption edge permits the recording of Bragg reflections with enhanced sensitivity to the specific ion and its electronic configuration. In the case of the Fe K edge, the incident x-rays virtually excite an electron from the 1s core level to the empty 4p states, followed by a decay of the electron back to the core hole. This effect results in a significant variation in the atomic scattering factors of the Fe ions for x-ray energies close to the Fe K edge. In particular, the atomic scattering factors are affected by variations in the charge state, as witnessed by a change in chemical shift. We report on the temperature dependence of the $(\frac{1}{3}\frac{1}{3}\frac{7}{2})$ reflection across T_N . This reflection has a strong resonance and is most sensitive to changes in the CO. A change in CO will change the functional form of the resonance. In addition any change in the Thomson scattering below and above the resonance signifies a change in the crystallographic distortion associated with the CO. In contrast to neutron diffraction, RXD at the Fe K edge is not sensitive to the magnetic order of the Fe ions.

II. EXPERIMENT

RXD measurements were performed at the Materials Science beam line at the Swiss Light Source using the Pilatus 2D detector⁴¹ and with the same sample of LuFe_2O_4 as used for the study in Ref. 36. The measurements were recorded at selected temperatures between 100 and 300 K using horizontal incident polarization. The background, mainly originating from the fluorescence of the sample, was determined from a selected outer rim of the area detector and subtracted from all the recorded profiles. Both the $(\frac{1}{3}\frac{1}{3}\frac{7}{2})$ charge order reflection and the (006) structural reflection were recorded for each temperature, and the latter was used to perform absorption correction of the former according to the following procedure. The scattering factor of the (006) is expressed as $F(E) = \sum_j [f_{0,j} + f'_j(E) + if''_j(E)]e^{i\mathbf{q}\cdot\mathbf{r}_j}$ where $f_{0,j}$ is the atomic form factor and f'_j and f''_j are real and imaginary anomalous x-ray scattering factors of atom j , respectively; \mathbf{q} is the scattering vector; and \mathbf{r}_j is the position of atom j in the unit cell. The absorption is proportional to f''/E according to the optical theorem and was obtained from the (006) reflection by iteration of the calculated anomalous intensity according to space group $R\bar{3}m$ and the absorption deduced from the ratio between calculated and integrated intensity. The Kramers-Kronig transformation was performed with DIFFKK software from the IFEFFIT package,⁴² and the initial values of the anomalous scattering factors of Fe were the Cromer-Lieberman values obtained from DIFFKK. Figure 1(a) shows f'' obtained from this iterative process for $T = 100$ and $T = 300$ K. The intensity of the $(\frac{1}{3}\frac{1}{3}\frac{7}{2})$ reflection was in addition corrected for a small background, and the corrected resonance profiles are shown in Fig. 1(b).

III. RESULTS

Figure 1(b) shows the normalized integrated resonant diffraction intensity of the $(\frac{1}{3}\frac{1}{3}\frac{7}{2})$ reflection as a function of energy. We find that the functional form and the relative amplitude of the resonance are identical for all temperatures. Figure 1(b) indicates the features in the resonance curve labeled A and B. These two peaks are the most prominent part of each resonant intensity curve and have a Gaussian-type shape that is reproducible between measurements. The inset in Fig. 1 shows the integrated intensity of the $(\frac{1}{3}\frac{1}{3}\frac{7}{2})$ reflection as a function of temperature, normalized at $T = 100$ K. The integrated intensity increases gradually with decreasing temperature, remains nearly constant below $T = 200$ K, and shows a slight anomaly near T_N .

In addition to the measurements after zero-field cooling (ZFC), the LuFe_2O_4 sample was heated *ex situ* to $T = 350$ K and cooled in an applied electric field of 250 kV/m along the [001] direction to $T = 300$ K, followed by RXD at selected temperatures between 150 and 300 K. The procedure was then repeated with the electric field along the $[00\bar{1}]$ direction. Because of the remounting of the sample, absolute intensities could not be compared. However, the energy dependencies of the $(\frac{1}{3}\frac{1}{3}\frac{7}{2})$ reflection recorded for the positive electric field cooled (+EFC) and negative electric field cooled (−EFC) sample were qualitatively the same as the ZFC results, as shown in Fig. 1(b).

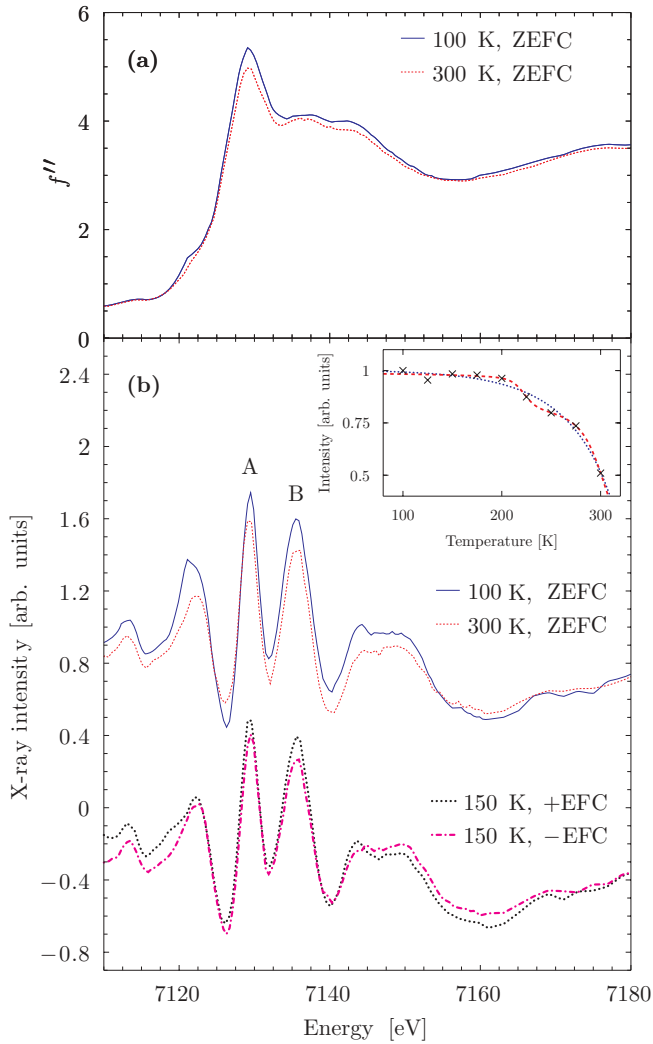


FIG. 1. (Color online) (a) $f''(E)$ deduced from the integrated intensity of the (006) reflection (see text) as a function of x-ray energy. (b) Integrated resonant diffraction intensity of the $(\frac{1}{3}\frac{1}{3}\frac{7}{2})$ reflection at the Fe K edge as a function of x-ray energy. The integrated intensity is normalized and corrected for absorption. The two peaks used in the data analysis are labeled A and B. The integrated resonant diffraction intensity profiles measured after +EFC and -EFC are shifted downwards for clarity. The inset shows the intensity of the $(\frac{1}{3}\frac{1}{3}\frac{7}{2})$ superstructure reflection as a function of temperature (error bars are less than the size of the symbols). The lines added as guides for the eye are obtained from a fit with a Brillouin curve (blue dotted line) and with a sum of two Brillouin curves (red dashed line). The intensities shown in the inset have not been corrected for absorption.

IV. DISCUSSION

The charge order in LuFe_2O_4 coincides with a crystallographic distortion resulting in the Thomson intensity. A change in charge order is therefore likely to concur with a change in the crystallographic distortion. Using the anomalous scattering factors of Fe^{2+} and Fe^{3+} determined in Ref. 36, the energy dependency of the $(\frac{1}{3}\frac{1}{3}\frac{7}{2})$ reflection was calculated for two scenarios of charge disproportionation, one coinciding with crystallographic distortion, the other without.

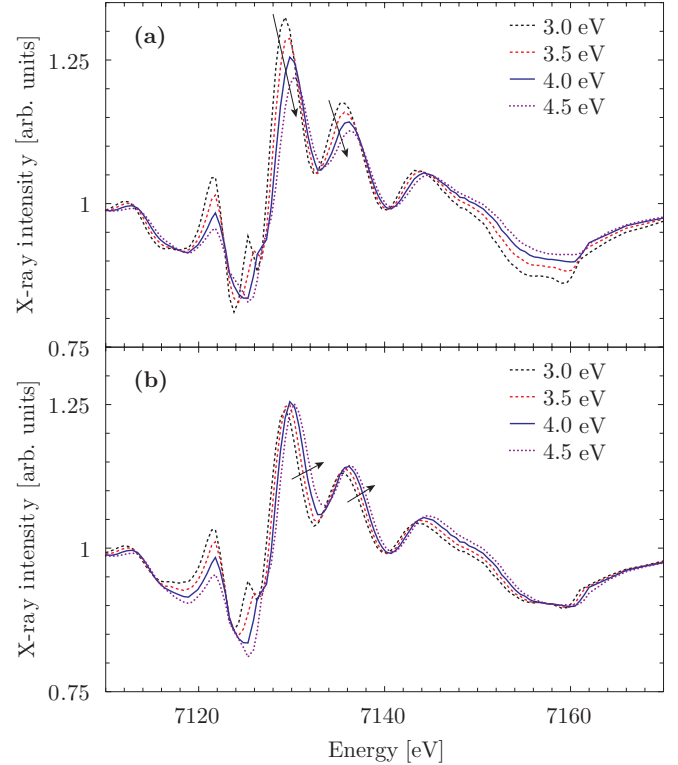


FIG. 2. (Color online) Calculated XRD intensity of the CO reflection $(\frac{1}{3}\frac{1}{3}\frac{7}{2})$ as a function of the chemical shift with (a) constant Thomson scattering and (b) Thomson scattering proportional to δ^2 . The case of (a) corresponds to the change of partial charge only, and (b) assumes an accompanying structural distortion.

The chemical shift Δ between the two iron species is typically proportional to the charge disproportionation and was varied from $\Delta = 3$ to 4.5 eV, which corresponded to a change in charge disproportionation of $0.19e$. The Thomson intensity was (a) kept constant [see Fig. 2(a)] as well as (b) varied proportionally to δ^2 [see Fig. 2(b)]. The first simulates charge disproportionation at the Fe sites while the crystal distortion remains constant, while the latter simulates charge disproportionation that is proportional to the crystallographic distortion.

It becomes apparent that regardless of the assumed presence of lattice distortion or lack of it, the change in Δ results in a change of position of resonant peaks A and B that is significant and similar in cases (a) and (b). An increase of the chemical shift Δ between the two iron species by 1 eV results in a shift of 0.63 and 0.61 eV for peaks A and B, respectively, in both (a) and (b). Therefore, in the data analysis we examine the resonant peak positions with temperature to detect possible changes in Δ .

To determine the positions of A and B, the peaks were fitted with a sum of Gaussian and linear functions. Figure 3 illustrates that the positions of A (red crosses) and B (blue diagonal crosses) are constant as a function of temperature. Their variability is compared to the change in position that corresponds to a 1 eV change in Δ (black lines), based on the simulated resonance profiles shown in Fig. 2. Using a linear relationship between Δ and δ results in a distribution

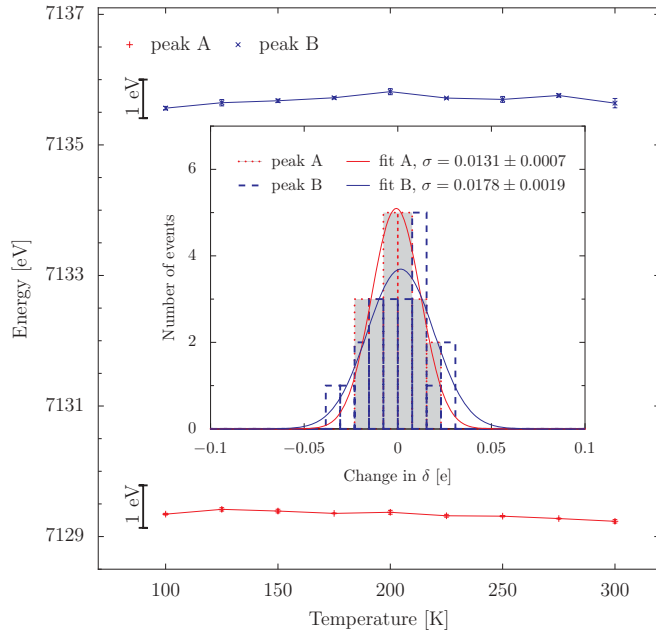


FIG. 3. (Color online) Positions of XRD peaks A and B as a function of temperature. The black line next to each data set shows the shift of peak position that corresponds to a 1-eV change in the chemical shift between the two iron sites. The inset shows the distribution of all the measured peak positions and the corresponding variation of δ . The distribution of the points indicates that the change of δ throughout all temperatures is less than $0.02e$ (4%).

of observed δ values as shown in the inset of Fig. 3. It is concluded that the charge disproportionation is independent of temperature within 4%. This upper limit of $0.02e$ is insufficient to account for the observed increase in polarization at T_N .

This confirms that the Coulomb interaction is dominant in LuFe_2O_4 as the charge disproportionation is complete both in the paramagnetic and ferrimagnetic states. This is in contrast to the stripe order observed in the hole doped perovskite family LaFeO_3 where the superexchange gives rise to different domain wall patterns of the charge density wave depending on the hole doping. In this case the charge and magnetic order are dominated by the magnetic exchange interaction rather than Coulomb interactions.^{43,44} Kajimoto *et al.* observe in $\text{Nd}_{1/3}\text{Sr}_{2/3}\text{FeO}_3$ a distinct temperature dependence between the spin and charge order superlattices with neutron diffraction and suggest that the magnetic moments on the Fe^{3+} and Fe^{5+} increase and decrease, respectively, when the charge disproportionation is close to complete.⁴⁵

The inset of Fig. 1(b) shows a gradual decrease in intensity of about 50% between $T = 100$ and $T = 300$ K. This is attributed to an increased probability of electron hopping between Fe sites.²⁹ As the time scale of RXD for virtual electron excitation at the Fe K edge (order of 10^{-16} s)⁴⁶ is smaller than the rate of electron hopping (5×10^{-6} s at $T = 330$ K),²⁹ RXD provides a snapshot of the charge order. Thus there is an increase in the number of Fe sites that are populated randomly by either Fe^{2+} or Fe^{3+} as function of temperature. These sites do not take part in the charge

ordered superstructure, therefore reducing the intensity of the CO reflection. An increase of the effective number or the probability of electrons that are hopping from Fe^{2+} to Fe^{3+} sites has also been observed with optical spectroscopy²⁹ and is consistent with our observations.

Previous studies have demonstrated pancakelike charge ordered domains in RFe_2O_4 (Ref. 30) that are also seen in the magnetic state of LuFe_2O_4 .³² Our findings suggest that the charge order in these domains is unchanged, while their number and size decreases with increasing temperature.

The inset of Fig. 1(b) compares the intensity of the CO reflection with two guides to the eye. The blue dotted line is the temperature dependence expected for a gradual increase in CO while the red dashed line includes an additional anomaly at T_N . The latter suggests a decrease in the probability of electron hopping due to the onset of magnetic ordering. This is consistent with stabilization of the CO due to the magnetic order as suggested by Nagano *et al.* in Ref. 26. It is also in agreement with our earlier neutron diffraction study,⁴⁰ where we show that the CO is stabilized in the magnetic state. The antiferromagnetic alignment of the Fe moments prevents the double exchange mechanism and reduces the probability for electrons to hop. We note however the limited number of data points as a function of temperature as well as the limited agreement of the intensity recorded at $T = 125$ K with either guide to the eye.

V. CONCLUSION

The temperature dependence of the CO reflection ($\frac{1}{3}\frac{1}{3}\frac{7}{2}$) has been investigated with resonant x-ray diffraction at the Fe K edge. The energy dependence is compared to two models of charge disproportionation, one including a lattice distortion, the other without. It is found that the change in charge disproportionation across T_N is less than $0.02e$. These findings suggest that the charge disproportionation between Fe^{2+} and Fe^{3+} is largely independent of temperature and the same for the ferroelectric and magnetic phase of LuFe_2O_4 . The intensity of the CO reflection decreases with temperature because of a growing probability of electron hopping that adds disorder in the charge order superstructure. The increase in polarization in the magnetic phase is therefore not of static origin and likely of a dynamic nature. The anomaly at T_N is consistent with the antiferromagnetic alignment of spins that reduces the probability of electron hopping as the double exchange mechanism is inhibited.

ACKNOWLEDGMENTS

We thank the beam line staff of X04SA and, in particular, Phil Willmott, for their excellent support, and Cristian Batista for a valuable discussion. This work was partly performed at the SLS of the Paul Scherrer Institut, Villigen, Switzerland. We acknowledge financial support from the International Synchrotron Access Programme of the Australian Government, NCCR MaNEP, and the Swiss National Science Foundation.

- ¹N. Kimizuka and T. Katsura, *J. Solid State Chem.* **13**, 176 (1975).
- ²K. Kato, I. Kawada, N. Kimizuka, and T. Katsura, *Z. Kristallogr.* **141**, 314 (1975).
- ³M. Tanaka, M. Kato, N. Kimizuka, and K. Siratori, *J. Phys. Soc. Jpn.* **47**, 1737 (1979).
- ⁴M. Tanaka, K. Siratori, and N. Kimizuka, *J. Phys. Soc. Jpn.* **53**, 760 (1984).
- ⁵J. Akimitsu, Y. Inada, K. Siratori, I. Shindo, and N. Kimizuka, *Solid State Commun.* **32**, 1065 (1979).
- ⁶M. Tanaka, H. Iwasaki, K. Siratori, and I. Shindo, *J. Phys. Soc. Jpn.* **58**, 1433 (1989).
- ⁷N. Ikeda, K. Saito, K. Kohn, H. Kito, J. Akimitsu, and K. Siratori, *Ferroelectrics* **161**, 111 (1994).
- ⁸N. Ikeda, K. Kohn, H. Kito, J. Akimitsu, and K. Siratori, *J. Phys. Soc. Jpn.* **63**, 4556 (1994).
- ⁹Y. Yamada, S. Nohdo, and N. Ikeda, *J. Phys. Soc. Jpn.* **66**, 3733 (1997).
- ¹⁰Y. Yamada, K. Kitsuda, S. Nohdo, and N. Ikeda, *Phys. Rev. B* **62**, 12167 (2000).
- ¹¹Y. Yamada, O. Hino, S. Nohdo, R. Kanao, T. Inami, and S. Katano, *Phys. Rev. Lett.* **77**, 904 (1996).
- ¹²C. H. Chen, S.-W. Cheong, and A. S. Cooper, *Phys. Rev. Lett.* **71**, 2461 (1993).
- ¹³N. Ikeda, H. Ohsumi, K. Ohwada, K. Ishii, T. Inami, K. Kakurai, Y. Murakami, K. Yoshii, S. Mori, Y. Horibe, and H. Kito, *Nature (London)* **436**, 1136 (2005).
- ¹⁴N. Ikeda, M. Kubota, H. Hayakawa, H. Akahama, D. Ohishi, A. Nakanishi, T. Funabiki, Y. Matsuo, N. Kimizuka, T. Kambe, S. Mori, and J. Kano, *Ferroelectrics* **414**, 41 (2011).
- ¹⁵B. Fisher, J. Genossar, L. Patlagan, and G. M. Reisner, *J. Appl. Phys.* **109**, 084111 (2011).
- ¹⁶M. Subramanian, T. He, J. Chen, N. Rogado, T. Calvarese, and A. Sleight, *Adv. Mater.* **18**, 1737 (2006).
- ¹⁷J. Wen, G. Xu, G. Gu, and S. M. Shapiro, *Phys. Rev. B* **80**, 020403 (2009).
- ¹⁸C.-H. Li, F. Wang, Y. Liu, X.-Q. Zhang, Z.-H. Cheng, and Y. Sun, *Phys. Rev. B* **79**, 172412 (2009).
- ¹⁹F. Wang, C.-H. Li, T. Zou, Y. Liu, and Y. Sun, *J. Phys.: Condens. Matter* **22**, 496001 (2010).
- ²⁰P. Ren, Z. Yang, W. G. Zhu, C. H. A. Huan, and L. Wang, *J. Appl. Phys.* **109**, 074109 (2011).
- ²¹J. Wen, G. Xu, G. Gu, and S. M. Shapiro, *Phys. Rev. B* **81**, 144121 (2010).
- ²²J. de Groot, K. Marty, M. D. Lumsden, A. D. Christianson, S. E. Nagler, S. Adiga, W. J. H. Borghols, K. Schmalzl, Z. Yamani, S. R. Bland, R. de Souza, U. Staub, W. Schweika, Y. Su, and M. Angst, *Phys. Rev. Lett.* **108**, 037206 (2012).
- ²³N. Ikeda, *J. Phys.: Condens. Matter* **20**, 434218 (2008).
- ²⁴M. Phan, N. Frey, M. Angst, J. de Groot, B. Sales, D. Mandrus, and H. Srikanth, *Solid State Commun.* **150**, 341 (2010).
- ²⁵M. Angst, R. P. Hermann, A. D. Christianson, M. D. Lumsden, C. Lee, M.-H. Whangbo, J.-W. Kim, P. J. Ryan, S. E. Nagler, W. Tian, R. Jin, B. C. Sales, and D. Mandrus, *Phys. Rev. Lett.* **101**, 227601 (2008).
- ²⁶A. Nagano, M. Naka, J. Nasu, and S. Ishihara, *Phys. Rev. Lett.* **99**, 217202 (2007).
- ²⁷M. Naka and S. Ishihara, *J. Phys.: Conference Series* **320**, 012083 (2011).
- ²⁸A. D. Christianson, M. D. Lumsden, M. Angst, Z. Yamani, W. Tian, R. Jin, E. A. Payzant, S. E. Nagler, B. C. Sales, and D. Mandrus, *Phys. Rev. Lett.* **100**, 107601 (2008).
- ²⁹X. S. Xu, M. Angst, T. V. Brinzari, R. P. Hermann, J. L. Musfeldt, A. D. Christianson, D. Mandrus, B. C. Sales, S. McGill, J.-W. Kim, and Z. Islam, *Phys. Rev. Lett.* **101**, 227602 (2008).
- ³⁰Y. Murakami, N. Abe, T. Arima, and D. Shindo, *Phys. Rev. B* **76**, 024109 (2007).
- ³¹Y. Horibe, K. Yoshii, N. Ikeda, and S. Mori, *Phys. Rev. B* **80**, 092104 (2009).
- ³²S. Park, Y. Horibe, Y. J. Choi, C. L. Zhang, S.-W. Cheong, and W. Wu, *Phys. Rev. B* **79**, 180401 (2009).
- ³³J. A. Alonso, J. L. García-Muñoz, M. T. Fernández-Díaz, M. A. G. Aranda, M. J. Martínez-Lope, and M. T. Casais, *Phys. Rev. Lett.* **82**, 3871 (1999).
- ³⁴U. Staub, G. I. Meijer, F. Fauth, R. Allenspach, J. G. Bednorz, J. Karpinski, S. M. Kazakov, L. Paolasini, and F. d'Acapito, *Phys. Rev. Lett.* **88**, 126402 (2002).
- ³⁵V. Scagnoli, U. Staub, M. Janousch, A. M. Mulders, M. Shi, G. I. Meijer, S. Rosenkranz, S. B. Wilkins, L. Paolasini, J. Karpinski, S. M. Kazakov, and S. W. Lovesey, *Phys. Rev. B* **72**, 155111 (2005).
- ³⁶A. M. Mulders, S. M. Lawrence, U. Staub, M. Garcia-Fernandez, V. Scagnoli, C. Mazzoli, E. Pomjakushina, K. Conder, and Y. Wang, *Phys. Rev. Lett.* **103**, 077602 (2009).
- ³⁷M. Benfatto, J. A. Solera, J. G. Ruiz, and J. Chaboy, *Chem. Phys.* **282**, 441 (2002).
- ³⁸X. S. Xu, J. de Groot, Q.-C. Sun, B. C. Sales, D. Mandrus, M. Angst, A. P. Litvinchuk, and J. L. Musfeldt, *Phys. Rev. B* **82**, 014304 (2010).
- ³⁹J. de Groot, T. Mueller, R. A. Rosenberg, D. J. Keavney, Z. Islam, J.-W. Kim, and M. Angst, *Phys. Rev. Lett.* **108**, 187601 (2012).
- ⁴⁰A. M. Mulders, M. Bartkowiak, J. R. Hester, E. Pomjakushina, and K. Conder, *Phys. Rev. B* **84**, 140403 (2011).
- ⁴¹C. Broennimann, E. F. Eikenberry, B. Henrich, R. Horisberger, G. Huelsen, E. Pohl, B. Schmitt, C. Schulze-Briese, M. Suzuki, T. Tomizaki, H. Toyokawa, and A. Wagner, *J. Synchrotron Radiat.* **13**, 120 (2006).
- ⁴²M. Newville, *J. Synchrotron Radiat.* **8**, 96 (2001).
- ⁴³R. J. McQueeney, J. Ma, S. Chang, J.-Q. Yan, M. Hehlen, and F. Trouw, *Phys. Rev. Lett.* **98**, 126402 (2007).
- ⁴⁴T. Mizokawa and A. Fujimori, *Phys. Rev. Lett.* **80**, 1320 (1998).
- ⁴⁵R. Kajimoto, Y. Oohara, M. Kubota, H. Yoshizawa, S. Park, Y. Taguchi, and Y. Tokura, *J. Phys. Chem. Solids* **62**, 321 (2001).
- ⁴⁶H. Renevier, Y. Joly, J. Garca, G. Subas, M. G. Proietti, J. L. Hodeau, and J. Blasco, *J. Synchrotron Radiat.* **8**, 390 (2001).